

Effect of Weathering on the Mineralogy and Geochemistry of Sediments of the Hyper Saline Urmia Salt Lake, Iran

Samad Alipour, Khadije Mosavi Onlaghi

Abstract—Urmia Salt Lake (USL) is a hypersaline lake in the northwest of Iran. It contains halite as main dissolved and precipitated mineral and the major mineral mixed with lake bed sediments. Other detrital minerals such as calcite, aragonite, dolomite, quartz, feldspars, augite are forming lake sediments. This study examined the impact of weathering of this sediments collected from 1.5 meters depth and augite placers. The study indicated that weathering of tephritic and adakite rocks of the Islamic Island at the immediate boundary of the lake play a main control of lake bed sediments and has produced a large volume of augite placer along the lake bank. Weathering increases from south to toward north with increasing distance from Islamic Island. Geochemistry of lake sediments demonstrated the enrichment of MgO, CaO, Sr with an elevated anomaly of Eu, possibly due to surface absorbance of Mn and Fe associated Sr elevation originating from adakite volcanic rocks in the vicinity of the lake basin. The study shows the local geology is the major factor in origin of lake sediments than chemical and biochemical produced mineral during diagenetic processes.

Keywords—Urmia Lake, weathering, mineralogy, augite, Iran.

I. INTRODUCTION

USL consists of 5200-6000 km² and 65×10⁸ tons of pure salt and tremendous amount of thick bed sediments [1], now exposed to the air. Weathering of these sediments can play an important role in clarifying environmental geochemistry of USL bed sediments. The sediments could display their geochemical controlled factors such as source rocks, weathering, geochemical processes, transportation, and diagenetic phenomena [2]-[6]. Understanding major, trace and rare earth elements' (REE) behavior in sediments in water systems have been previously described [7]-[10]. The weathering impact on the sediments composition from the northeast bank of USL is forming the main aim of this research.

II. METHODOLOGY

Mineralogical and geochemical analyses were performed for 17 samples taken from 1.5 meters depth by hand auger. 14 samples were analyzed by XRF and ICP-MS for major trace and rare earth elements. Four samples were also investigated by XRD for mineral identification phases.

Samad Alipour and Khadije Mosavi Onlaghi are with the Department of Geology, Faculty of Sciences, University of Urmia, Urmia, Iran (e-mail: s.alipour@urmia.ac.ir, mosavi48ksh@gmail.com).

III. GEOLOGY

Geological formations surrounding the lake consist of Jurassic, Cretaceous shale and limestone and Eocene Volcanic rocks [1] (Fig. 1) occupying up to 500 km² agglomeratic of tephrite, basanite with pyroclastic interlayer and tuffaceous weathered materials [11], (Figs. 2 (a), (b)) known as Islamic island. Sediment types of the USL may have been controlled by factors such as geochemistry of the material, physical and chemical basin weathering, sedimentation and diagenetic processes [12]. The Islamic Island in the northeastern part is a unique geological character of the area. Augite is the main mineral forming a large volume of augite placer (Fig. 3) along the north-east bank of USL (Fig. 1).

IV. MINERALOGY

XRD results (Table I) show augite and halite as the main mineral phases (Figs. 4 (a), (b)), associated with clastic and pyroclastics materials from mid-east to north (Fig. 1), (Agh-Gonbad to Taymorloo villages around the Aji-Chay river). Minor minerals at the studied profile (Fig. 1) consist of aragonite, calcite, muscovite-illite, chlorite, quartz, albite, hornblende, carbonate-hydroxide-apatite.

Overall, sediments can be grouped in two categories including clastic and chemical/biochemical, similar to previous reports from the south-west [14] and south-east of USL [15].

Clastic sediments include volcanic silicates such as augite, hornblende, quartz, albite and clays including muscovite and illite. Illite is an abundant clay mineral in the sediments possibly formed from weathering of feldspatoides or muscovite [16] of rocks from Islamic Island.

Following the increase of Mg concentration in the lake during the last 20 years [17], Dolomite and calcite may have been precipitated in-situ as well as being carried to the lake by rivers. Some minerals such as ankerite, aragonite, halite and calcite are associated with minor phase such as albite, gypsum, montmorillonite, dolomite, chlorite and muscovite (Table I and Figs. 5 (a), (b)). This indicates that the local geology is the main controlling factor of the chemical composition of the lake bed sediments, rather than chemical precipitation within the lake, as demonstrated by previous works of in the south-east [15] and south west [14] banks of USL.

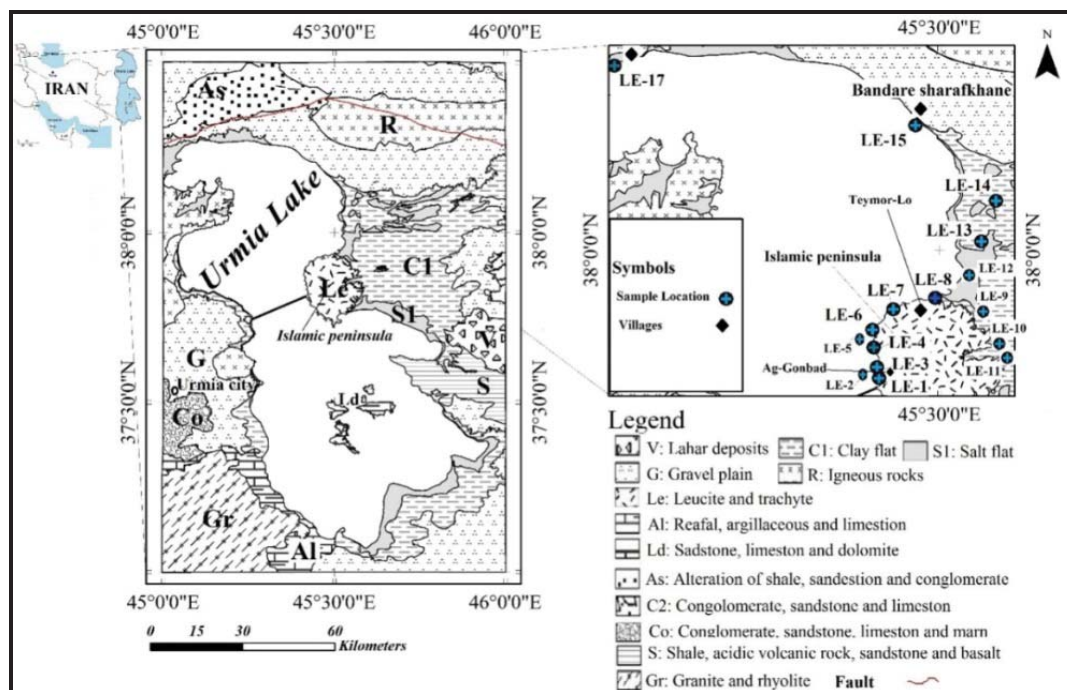


Fig. 1 Geological map of the USL with sample location [13]



Fig. 2 Volcanic flow structure of the Islamic Island nearby the Kalantary causeway (a) and Agh-Gonbad village (b)

TABLE I
MAJOR AND MINOR MINERAL PHASES OF LAKE BAD SEDIMENTS BY XRD ANALYSIS

Sample number	Major phase	Minor phase
LE-1	Halite (NaCl)	Aragonite (CaCO_3)
		Calcite (CaCO_3)
		Muscovite-illite ($\text{KAl}_2\text{Si}_3\text{AlO}_{10}(\text{OH})_2$)
		Chlorite ($\text{Mg}_6\text{Fe}_6(\text{Si}_4\text{Al})_4\text{O}_{10}(\text{OH})_8$)
LE-4	Augite ($\text{Ca}(\text{Fe},\text{Mg})\text{Si}_2\text{O}_6$)	Hornblende ($\text{Ca}_2(\text{Fe},\text{Mg})_4\text{Al}(\text{Si}_7\text{Al})\text{O}_{22}(\text{OH})_2$)
		Carbonate-hydroxide-apatite ($\text{Ca}_{10}(\text{PO}_4)_3(\text{CO}_3)_3(\text{OH})_2$)
LE-5	Ankerite $\text{Ca}(\text{Fe},\text{Mg})(\text{CO}_3)_2$	Aragonite (CaCO_3)
	Halite (NaCl)	Albite ($\text{NaAlSi}_3\text{O}_8$)
	Calcite (CaCO_3)	Gypsum ($\text{CaSO}_4 \cdot 2\text{H}_2\text{O}$)
	Quartz (SiO_2)	Montmorillonite $\text{CaO}_2(\text{Al},\text{Mg}_2\text{Si}_4\text{O}_{10}(\text{OH})_2 \cdot \text{XH}_2\text{O})$
LE-15	Halite (NaCl)	Calcite (CaCO_3)
	Aragonite	Muscovite-illite ($\text{KAl}_2\text{Si}_3\text{AlO}_{10}(\text{OH})_2$) ₆
	Quartz (SiO_2)	chlorite ($\text{Mg}_6\text{Fe}_6(\text{Si}_4\text{Al})_4\text{O}_{10}(\text{OH})_8$)
	Calcite (CaCO_3)	Dolomite ($\text{CaMg}(\text{CO}_3)_2$)
		Albite ($\text{NaAlSi}_3\text{O}_8$)

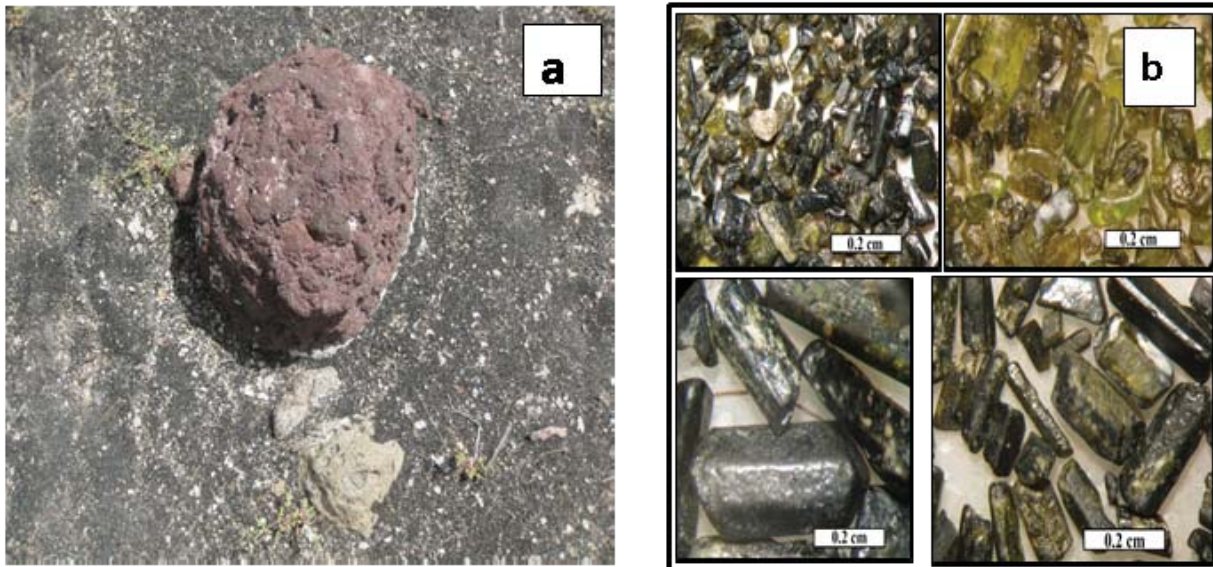


Fig. 3 Augite placer (a) and picture of Augite crystals under microscope STME SV8 (b)

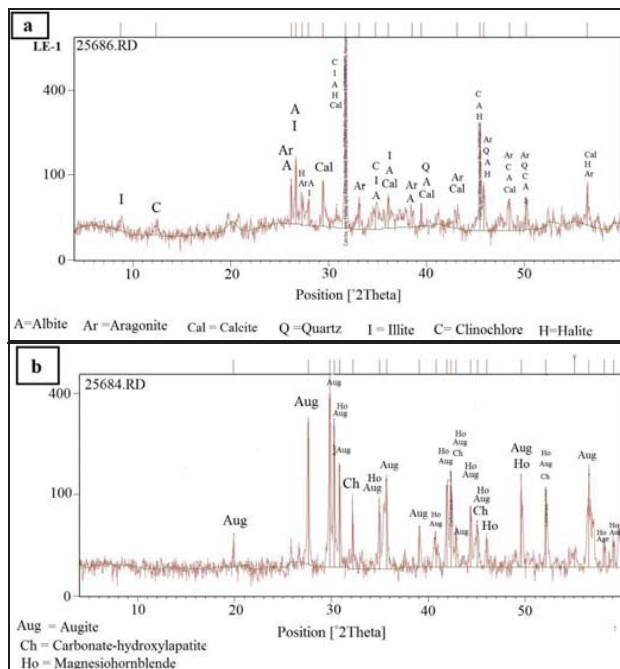


Fig. 4 XRD diagrams of lake sediments mineralogy

V. ORIGIN OF SEDIMENTS

Geochemical diagrams of silica vs. the total alkalis (TAS), [18] represent basic to ultrabasic fields of foidite, tephrite (sample LE-8, 15, 17) to pirobasalt (LE-13-3-14) and basalt (LE-4, 7) for sediments (Fig. 6).

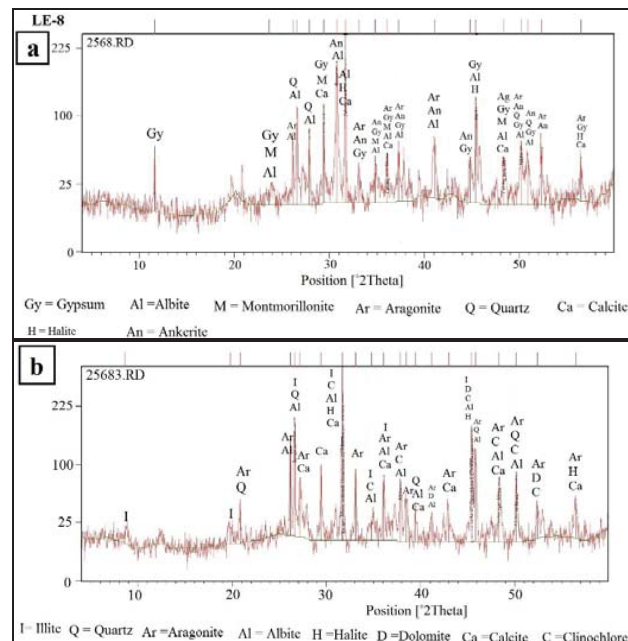


Fig. 5 XRD diagrams of lake sediments mineralogy

VI. WEATHERING

Two types of clay weathering index plots of $[Al_2O_3 - (Fe_2O_3 + MgO)]$ (Fig. 7 (a)) and $(CaO + Na_2O + K_2O)$, [19], [20], (Fig. 7 (b)) were used to determine weathering intensity. Result of both plots indicated (Fig. 7) increased weathering intensity toward the north, tending near the Al_2O_3 vertex and depletion from Ca, Na, and K due to longer transportation distances. Samples toward the south are enriched in elements such as Al_2O_3 . Al_2O_3 Increase toward the north (Figs. 6; 7 (a), (b)) associated with unaltered feldspars indicate relation the distance from Islamic island. The highest value is close to

Islamic island tephritic rocks, while lower values move toward north close to sedimentary clays of Aji-Chay with longer transported delta sediments.

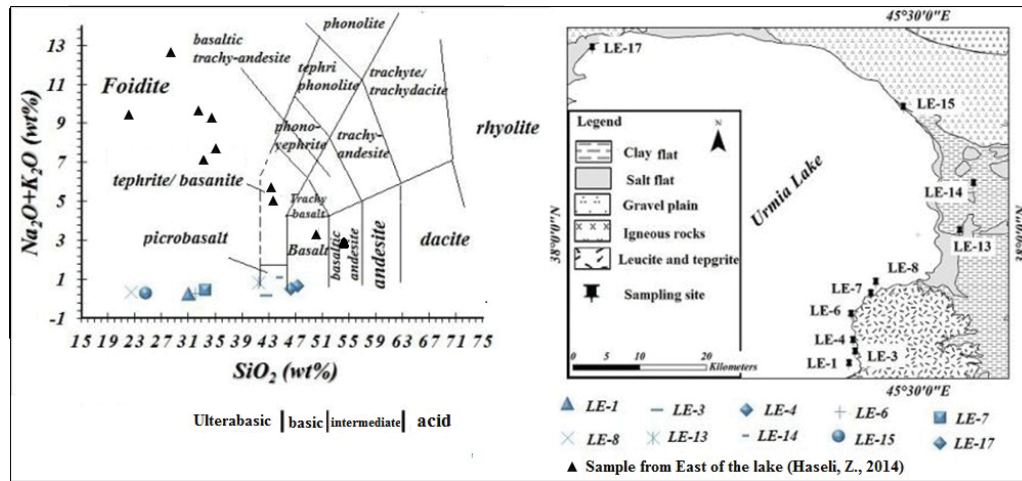


Fig. 6 Diagrams of rock origin of northeast and south east sediments of the lake (Including 10 samples from SE of the lake [15])

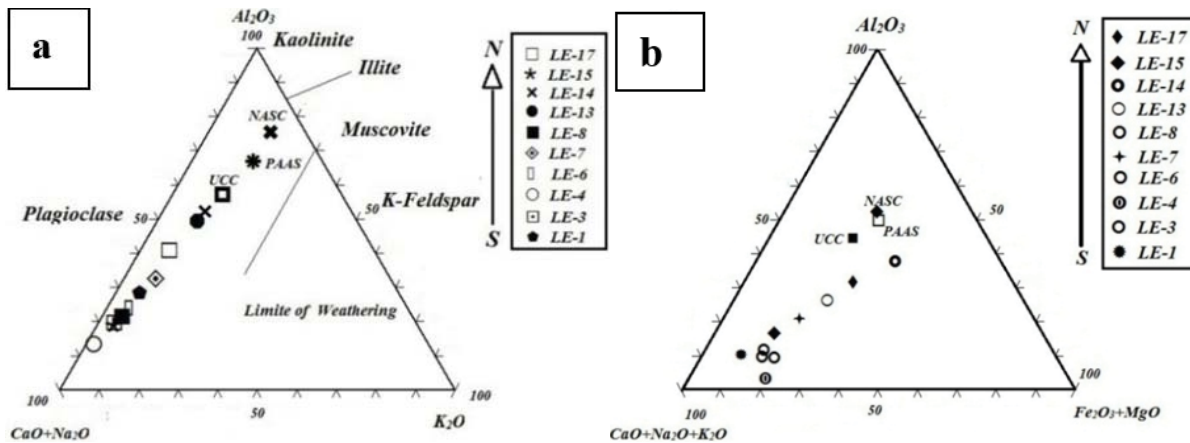


Fig. 7 Al_2O_3 -($CaO + Na_2O$)- K_2O plot of sediment samples [19], [20] compared to data for Post-Archean Average Shale (PAAS) and Upper Crust (UC) by [7] and North American Shale Composite (NASC) [21] (a). Triangular Al_2O_3 -($CaO+Na_2O+K_2O$)- Fe_2O_3+MgO plot of sediment samples [19], [20] in comparison with Post-Archean average shale and upper crust [7] and North American Shale Composite [21] (b)

In the " Fe_2O_3 - K_2O - Al_2O_3 " ternary plot [22], most of the samples plot close to the Al_2O_3 vertex, whereas some tephritic samples (LE-1-3-4-6) plot towards the Fe_2O_3 vertex (Fig. 8 (a)). Also, discriminant function diagram [23] indicates both mafic and silicate bimodal origin for analyzed samples (Fig. 8 (b)). Both of these figures demonstrate mixed clastic (transported from flowing rivers) and pyroclastic (from Islamic Island volcanic complex) sources.

- Discriminant function I = $-1.773 TiO_2 + 0.607 Al_2O_3 + 0.75 Fe_2O_3$ (total) $- 1.5 MgO + 0.616 CaO + 0.509 Na_2O - 1.224 K_2O - 9.09$;
- Discriminant function II = $0.445 TiO_2 + 0.07 Al_2O_3 - 0.25 Fe_2O_3$ (total) $- 1.142 MgO + 0.438 CaO + 1.475 Na_2O + 1.426 K_2O - 6.861$.

VII. MATURITY AND WEATHERING INTENSITY OF SEDIMENTS

Maturity and weathering of the sediments is determined by mobility of major elements, transportation and diagenetic processes [24]-[27]. Plotting the analytical results in log of SiO_2/Al_2O_3 versus log (Na_2O/K_2O) [25], [26], shows most of the samples fall on graywacke (Fig. 9 (a)) and shale (Fig. 9 (b)), indicating immature, sediments, which emphasizes the control of the local geology as the main contribution of lake sediments.

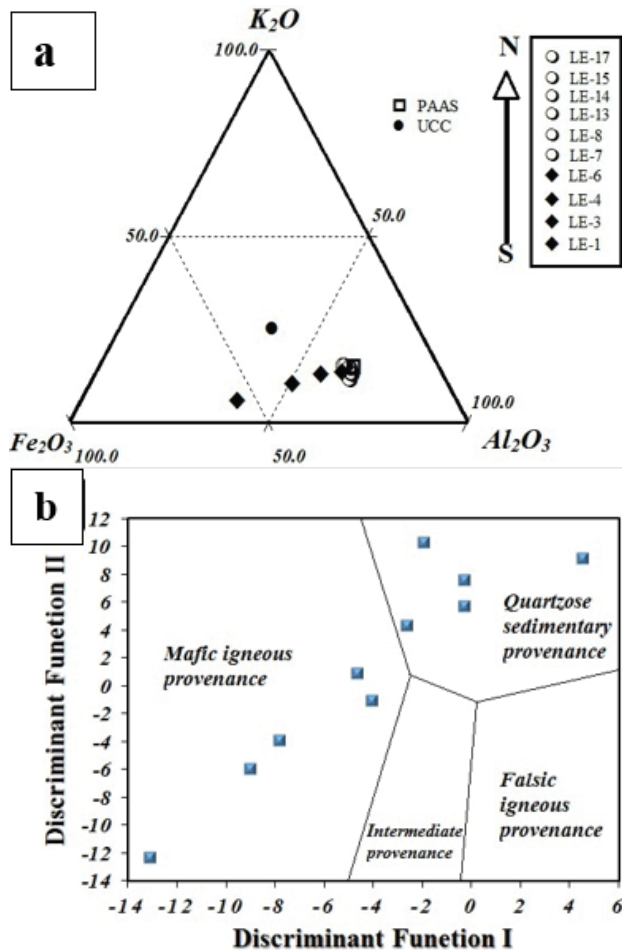


Fig. 8 Ternary plot of $(\text{Fe}_2\text{O}_3 - \text{K}_2\text{O} - \text{Al}_2\text{O}_3)$ [22] (a); Discriminant function diagram [23] (b) from the northeast part of the lake sediments

VIII. GEOCHEMISTRY

A. Geochemistry of Major Element

Strong enrichment of Ca, Na and Mg of major elements normalized to PAAS [7] (Fig. 10) and positive correlation between Fe_2O_3 with TiO_2 ($r=0.94$) and TiO_2 with MgO ($r=0.63$) in sediments (Table II) are indicating mafic composition, in compliance with the mafic source rocks of Islamic Island as strong influence of local geology contributing to the lake sediments.

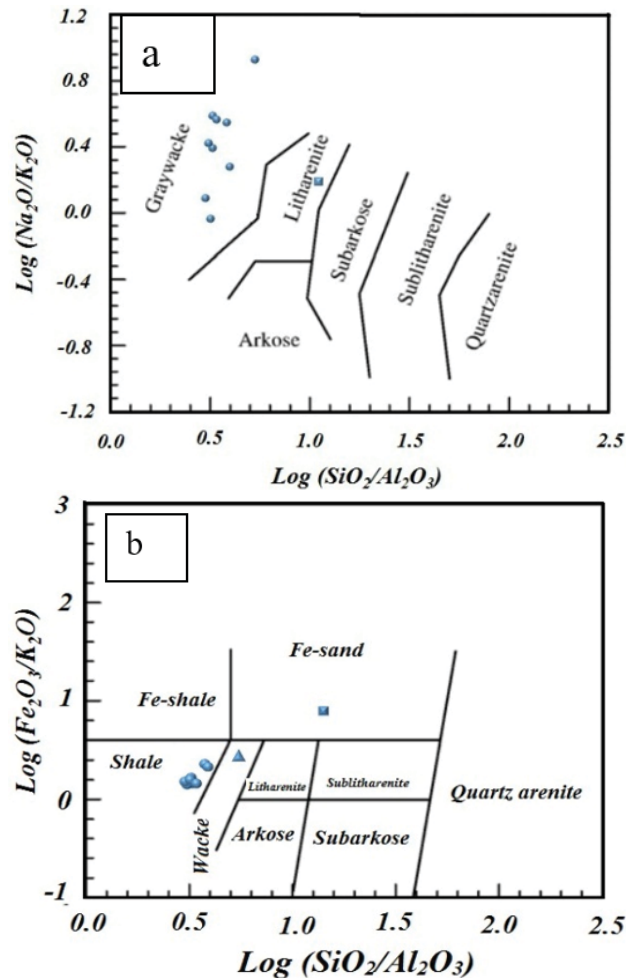


Fig. 9 Plots of $\text{Log} (\text{Na}_2\text{O}/\text{K}_2\text{O})$ and $\text{Log} (\text{Fe}_2\text{O}_3/\text{K}_2\text{O})$ vs. $\text{Log} (\text{SiO}_2/\text{Al}_2\text{O}_3)$ from USL sediments, following the geochemical classification diagrams [25] (a) and [26] (b)

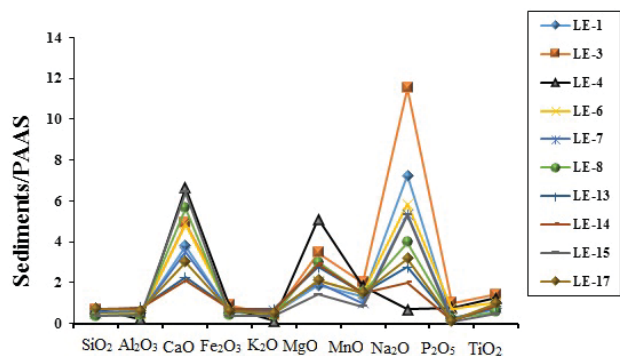


Fig. 10 Major oxides normalized to PAAS [7] variations in sampling profile of USL sediments

TABLE II
PEARSON CORRELATION BETWEEN MAJOR ELEMENTS OF LAKE BED SEDIMENTS OF THE NE PROFILE

	SiO ₂	Al ₂ O ₃	CaO	FeT	K ₂ O	MgO	MnO	Na ₂ O	P ₂ O ₅	TiO ₂
SiO ₂	1									
Al ₂ O ₃	0.263	1								
CaO	-0.395	-.964**	1							
FeT	.840**	0.093	-0.237	1						
K ₂ O	-0.013	.940**	-.886**	-0.075	1					
MgO	0.55	-0.417	0.297	0.608	-0.553	1				
MnO	0.61	-0.162	0.032	.783**	-0.338	.772**	1			
Na ₂ O	-0.255	-0.127	0.126	0.159	0.005	-0.289	0.101	1		
P ₂ O ₅	0.299	-0.558	0.44	.690*	-0.573	0.597	.718*	0.445	1	
TiO ₂	.750*	-0.162	0.004	.940**	-0.324	.639*	.833**	0.231	.830**	1

** . Correlation is significant at the 0.01 level (2-tailed). * . Correlation is significant at the 0.05 level (2-tailed).

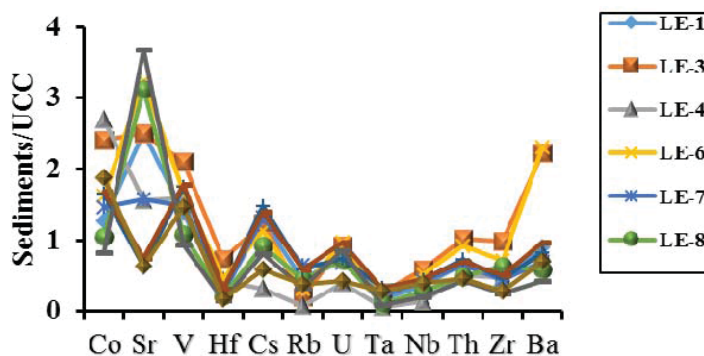


Fig. 11 Normalized trace elements distribution of northeast USL sediments to UCC [7]

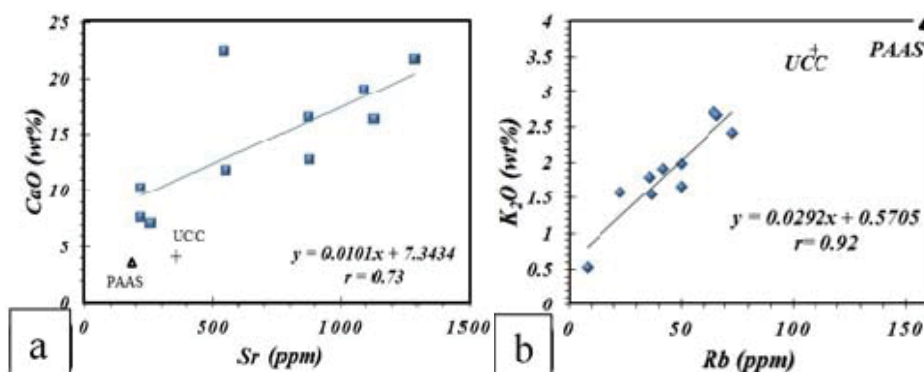


Fig. 12 Correlation equations between Sr and Ca (a) and Rb with K (b)

TABLE III
REEs OF SURFACE SEDIMENT SAMPLES FROM URMIA LAKE

Sample	LE-1	LE-3	LE-4	LE-6	LE-7	LE-8	LE-13	LE-14	LE-15	LE-17
La	21	41	31	34	22	17	23	24	14	18
Ce	41	84	67	66	43	36	44	46	28	35
Pr	4.97	11.31	9.82	8.39	5.12	3.86	5.14	5.33	3.21	4.32
Nd	19.9	48.2	43.9	33.8	20.2	15.3	19.8	20.5	12.6	17.1
Sm	3.81	10.26	9.84	6.72	3.86	2.85	3.81	3.98	2.35	3.37
Eu	0.97	2.68	2.56	1.81	0.98	0.73	0.97	0.98	0.58	0.95
Gd	3.09	8.09	7.95	5.26	3.2	2.33	3.29	3.38	1.97	3.05
Tb	0.45	1.08	1.1	0.72	0.49	0.36	0.52	0.52	0.32	0.48
Dy	2.52	5.84	5.59	3.8	2.72	1.94	2.98	3.13	1.75	2.92
Er	1.29	2.55	2.29	1.77	1.51	0.97	1.84	1.97	1.14	1.65
Tm	0.2	0.31	0.27	0.24	0.22	0.16	0.27	0.28	0.17	0.24
Yb	1.9	2.8	2.4	2.2	2.1	1.5	2.6	2.7	1.5	2.3
Lu	0.19	0.27	0.25	0.22	0.21	0.16	0.25	0.27	0.17	0.24
TREE	101.29	218.39	183.97	164.93	105.61	83.16	108.47	113.04	67.76	89.62
(La/Sm) _N	0.826	0.599	0.472	0.758	0.854	0.894	0.905	0.904	0.893	0.801
(Gd/Yb) _N	0.950	1.687	1.93	1.39	0.890	0.907	0.739	0.731	0.767	0.774
(Eu/Eu*)	0.861	1.45	1.41	1.21	0.856	0.747	0.847	0.837	0.646	0.870

TABLE IV
PEARSON CORRELATION BETWEEN MAJOR ELEMENTS WITH REES OF LAKE BED SEDIMENTS OF THE NE PROFILE

	SiO ₂	Al ₂ O ₃	CaO	FeT	K ₂ O	MgO	MnO	Na ₂ O	P ₂ O ₅	TiO ₂
La	0.458	-0.235	0.118	.845**	-0.271	0.529	.743*	0.431	.934**	.890**
Ce	0.452	-0.333	0.212	.832**	-0.373	0.607	.772**	0.407	.964**	.898**
Pr	0.494	-0.414	0.283	.832**	-0.478	.663*	.772**	0.349	.973**	.916**
Nd	0.493	-0.469	0.336	.814**	-0.539	.699*	.772**	0.321	.973**	.909**
Sm	0.512	-0.498	0.363	.807**	-0.58	.734*	.774**	0.279	.962**	.906**
Eu	0.515	-0.5	0.363	.804**	-0.586	.721*	.779**	0.282	.965**	.914**
Gd	0.555	-0.478	0.339	.826**	-0.574	.752*	.785**	0.246	.947**	.919**
Tb	0.598	-0.452	0.312	.843**	-0.561	.775**	.789**	0.196	.925**	.927**
Dy	.665*	-0.36	0.218	.893**	-0.489	.756*	.814**	0.209	.903**	.959**
Er	.828**	-0.018	-0.094	.974**	-0.19	.658*	.755*	0.118	.722*	.937**
Tm	.873**	0.252	-0.356	.972**	0.069	0.537	.706*	0.071	0.554	.868**
Yb	.881**	0.399	-0.504	.940**	0.215	0.464	.658*	0.021	0.433	.802**
Lu	.930**	0.347	-0.445	.926**	0.129	0.505	.651*	-0.068	0.416	.807**
Y	.718*	-0.238	0.098	.939**	-0.375	.724*	.821**	0.209	.869**	.974**

** . Correlation is significant at the 0.01 level (2-tailed).

*. Correlation is significant at the 0.05 level (2-tailed)

B. Geochemistry Trace Elements

Trace element patterns of the studied samples, normalized to UCC [7], [3], indicate enrichment of Sr and depletion of Rb, Ta and Hf (Fig. 11).

Sr levels in the SW and SE to the north of the causeway [14], [15] vary between 704 ppm and 1560 ppm respectively. The study area shows Sr levels between 222 and 1291 ppm with a mean value of 716 ppm which is enriched up to 3.5 times more than PAAS (200 ppm) and twice of UCC (350 ppm) all around the lake banks (Table III). This is a reflection of nearby adakitic volcanic rocks, characterized by Sr>400 ppm, SiO₂>56%, Al₂O₃>15%, MgO<3%, Y<18 ppm HREE, Yb<1.9 and have a high ratio of La/Yb>20 and Sr/Y>40 in the USL basin sediments [27].

Rubidium is rather limited in the adakitic surrounding rocks due to being hosted by insoluble rock forming minerals such as feldspars [28]-[30]. The ratio of Rb/Sr in the study area varies between 0.1 and 0.29 with a mean value of 0.1. This amount is less than of Rb/Sr mean in UCC (0.32) and of PAAS (0.8). The low ratio of Rb/Sr could be attributed to the abundance of Sr transportation from Sr rich tephrite and adakite from surrounding rocks of the watershed, rather than reflecting weathering intensity. Positive correlation between Rb with K₂O ($r=0.92$) is due to replacement in muscovite to and illite (Fig. 12 (a)), while positive correlation between Sr and CaO is indicative of Sr in calcite, aragonite and other Ca-chemical and biochemical minerals (Fig. 12 (b)).

C. Geochemistry Rare Earth Elements

In the NW of the lake, the concentration of REEs ranges from 67.75 to 218.38 ppm with the mean of 123.62 ppm, which is close to UCC (146.39 ppm), but it is less than 184.5 ppm of PAAS [7].

REEs normalized to UCC (Fig. 13) show an enrichment of LREEs (La/Sm)_n= 0.47-0.90 compared to HREEs (Gd/Yb)_n= 0.73-1.93 and positive Eu anomaly (Eu/Eu* = 0.64-3.18). REEs prefer to remain in organic phases as allochthonous compounds or attraction by oxides, clay minerals and organic

materials [31]-[33]. Positive trace elements correlation with REEs (Table IV) may be related to their similar behavior in this environment. Negative correlation of Rb ($r=-0.72$ to -0.13) and Sr ($r=-0.69$ to -0.15) with most REEs shows that the K and Ca-bearing minerals play a role in the REE concentration.

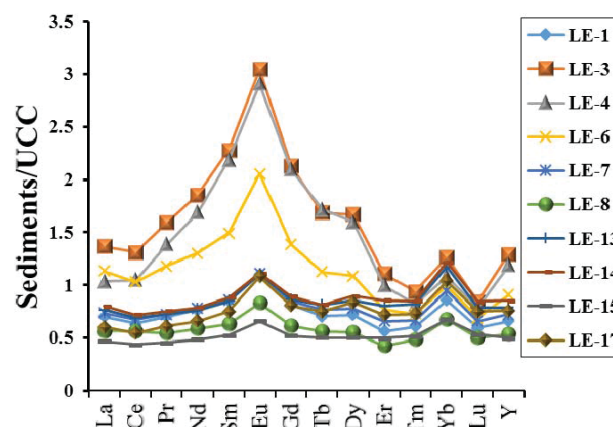


Fig. 13 REEs pattern of northeast USL sediments normalized to UCC [7] with distinctive Eu anomaly in augite abundant samples.

IX. CONCLUSION

- 1) The mineralogy of the lake sediments in the NE part of the USL, in spite of abundance of evaporative minerals, reflects the local geology. It is dominated by chemical and biochemical precipitates in the northern zone, while clastic minerals increase toward the southern part. Augite, as the main mineral forming the large placer, controls most of the trace and REEs in the sediments.
- 2) Lake sediments are enriched in Ca, Mg, Sr and Ba, but depleted in Rb, Ta and Hf with Sr depletion from augite-bearing samples. Sr in lake sediment is 3.5 times higher than of PAAS and twice of UCC. Strong correlation between Sr with CaO is due to replacement of Sr for Ca in carbonate minerals. Strong correlation between Rb with K is due to replacement of Rb for K₂O in illite-muscovite.

- 3) Rb/Sr (0.29-0.1) mean ratio in the profile is 0.1 which is less than that of UCC (0.32) and PAAS (0.8) and indicates the concentration of more Sr transported from Sr-rich tephritic rocks and probably intensive weathering.
- 4) REEs normalized to chondrite and UCC indicate the enrichments of LREEs compared to HREEs, associated with a positive Eu anomaly. Eu anomaly is controlled by the presence of augite and apatite while REEs are controlled by iron and manganese oxides surface attraction.
- 5) The local geology is the main control on forming the lake sediments rather than chemical precipitation of minerals from the lake water.

ACKNOWLEDGMENTS

The authors would like to acknowledge the financial support provided from Urmia University by the vice chancellor for research.

REFERENCES

- [1] Alipour S (2006). Hydrogeochemistry of seasonal variation of USL, Iran. *Saline Systems*. 2-9.
- [2] Bianchi TS, Mitra S, McKee BA (2002). Sources of terrestrially derived organic carbon in lower Mississippi River sediments: implications for differential sedimentation and transport at the coastal margin. *Mar Chem*. 77: 211-223.
- [3] Last WM and Smol JP (2001). *Tracking Environmental Change Using Lake Sediments*. Kluwer Academic Publishers, Dordrecht. The Netherlands.
- [4] Jin ZD, Wang S, Shen J, Wang Y (2003). Carbonate versus silicate Sr isotope in Lake sediments and its response to the Little Ice Age. *Chin. Sci Bull*. 48: 95-100.
- [5] Laird KR, Cumming BF, Wunsam S, Rusak JA, Oglesby RJ, Fritz SC, Leavitt PR (2003). Lake sediments record large-scale shifts in moisture regimes across the northern prairies of North America during the past two millennia. *Proc Natl Acad Sci*. 100: 2483-2488.
- [6] Rose, N.L., Boyle, J.F., Du, Y., Yi, C., Dai, X., Appleby, P.G., Bennion, H., Cai, S., Yu, L., 2004. Sedimentary evidence for changes in the pollution status of Taihu in the Jiangsu region of eastern China. *J. Paleolimnol*. 32, 41-51.
- [7] Taylor, S.R., McLennan, S.M., 1985. *The Continental Crust: Its Composition and Evolution*. Blackwell, London.
- [8] Knappe A, Möller P, Dulski P, Pekdeger A (2005). Positive gadolinium anomaly in surface water and ground water of the urban area Berlin. *Germany*. 65: 167-189.
- [9] Dupre B, Gaillardet J, Rousseau D, Allegre C (1995). Major and trace elements of river-borne material. *The Congo Basin*. 60: 1301-1321.
- [10] Elderfield H, Upstill-Goddard R, Sholkovitz E (1990). The rare earth elements in rivers, estuaries and coastal seas and their significance to the composition of ocean water. 54: 971-991.
- [11] Moayyed M, Moazzen M, Calagari AA, Jahangiri A, Modjarrad M (2008). Geochemistry and petrogenesis of lamprophyric dykes and the associated rocks from Eslamy peninsula, NW Iran: Implications for deep-mantle metasomatism. *Chemie der Erde*. 68: 141-154.
- [12] Fralick and Kronberg, 1997, Geochemical discrimination of elastic sedimentary rock sources, *sediment. Geol.* 113: 111-124.
- [13] Geological survey of Iran (GSI), 1:100000 national geochemical maps. (Adjabshir, 2005; Azarshahr, 2002; Marand, 1994; Oshnavieh, 1985, Tasodj, 1993; Urmia, 2006).
- [14] Hoseyni A (2012). Mineralogical and Geochemistry of SW corner of USL, M.Sc thesis, Urmia university.
- [15] Haseli Z (2014). Mineralogical and Geochemistry of SE corner of USL. M.Sc thesis. Urmia university.
- [16] Nelson, S.A., 2006, "Clay minerals", *Earth Materials*, 211 pp.
- [17] Sinha, R., Raymahashay, B., 2004. Evaporite mineralogy and geochemical evolution of the Sambhar Salt Lake, Rajasthan, India. *Sedimentary Geology*. 166, 59-71.
- [18] Le Maitre R W, Streckeisen A, Zanettin B, Le Bas M J, Bonin B, Bateman P, Bellieni G, Dudek A, Efremova S, Keller J, Lamere J, Sabine PA, Schmid R, Sorensen H, Wool A R (2002). *Igneous rocks*. A Classification and Glossary of Terms, in: Recommendation of the International Union of Geological Science Subcommittee on the systematics of Igneous rocks. 2nd Edn., Cambridge University Press. 254 pp.
- [19] Nesbitt, H. W. and Young, G. M., 1989. Formation and diagenesis of weathering profiles. *J. Geol.* 97, 129-147.
- [20] Nesbitt, H. W. and Young, G. M., 1996. Petrogenesis of sediments in the absence of chemical weathering: effects of abrasion and sorting on bulk composition and mineralogy. *Sedimentology*. 43, 341-358.
- [21] Gromet, L. P., Dymek, R. F., Haskin, L. A. and Korotev, R. L. (1984) The 'North American Shale Composite': its compilation, major and trace element characteristics. *Geochim. Cosmochim. Acta* 48, 2469-2482.
- [22] Condie KC (1993). Chemical composition and evolution of the upper continental crust: contrasting results from surface samples and shales. *Chemical Geology*. 104: 1-37.
- [23] Roser B. P., Korsch R. J., 1988. Provenance signatures of sandstone-mudstone suites determined using discriminant function analysis of major-element data. *Chem. Geol.* 67, 119-139.
- [24] McLennan S M, Hemming S, McDaniel DK, Hanson GN (1993). Geochemical approaches to sedimentation, provenance, and tectonics. *Processes Controlling the Composition of Clastic Sediments* (Johnson, M. J. and Basu, A., eds.). Geological Society of America. 284: 21-40.
- [25] Pettijohn, F.J., Potter, P.E., Siever, R., 1972. *Sand and Sandstone*. Springer-Verlag, New York.
- [26] Herron MM (1988). Geochemical classification of terrigenous sand and shales from core or log data. *J. Sediment. Petrol.* 58: 820-829.
- [27] Defant MJ, Drummond MS (1990). Derivation of some modern arc magmas by melting of young subducted. *Lithosphere Nature*. 367: 662-665.
- [28] Goldstein S, Jacobsen J (1988). Rare earth elements in river waters. *Sci Lett*. 89: 35-47.
- [29] Chen J, An Z, Head J (1999). Variation of Rb/Sr ratios in the loess paleosol sequences of central China during the last 130,000 year and their implications for monsoon paleoclimatology. *Quat.* 51: 215-219.
- [30] Yan Zeng, Jingan Chen, Jule Xiao, Liang Qi (2013). Non-residual Sr of the sediments in Daihai Lake as a good indicator of chemical weathering. *Quaternary Research*. 79: 284-291.
- [31] Ohta, A., Kawabe, I., 2001. REE (III) adsorption onto Mn dioxide (δ -MnO₂) and Fe oxyhydroxide: Ce (III) oxidation by δ -MnO₂. *Geochim. Cosmochim.* 65 (5), 695-703.
- [32] Coppin F, Berger G, Bauer A, Caste S, Loubet M (2002). Sorption of lanthanides on opectate and kaolinite. *Chem Geol.* 182: 57-68.
- [33] Haley BA, Klinkhammer GP, McManus J (2004). Rare earth elements in pore waters of marine sediments. *Geochim Cosmochim.* 68: 1265-1279.